

Effect of Modified Casting Process on Toughness and Wear Resistance of LM25 Alloy

Sunil Manani¹  · Nikunj Patel¹ ·
Ajaya Kumar Pradhan¹

Received: 10 May 2022 / Accepted: 12 November 2022 / Published online: 27 November 2022
© The Indian Institute of Metals - IIM 2022

Abstract The present research investigates the effect of a modified casting process along with/without Sr-modification on toughness and wear resistance of LM25 alloy. The results have revealed that the modified casting process reduces the size of α -Al grains and that of the eutectic Si particles without any morphological transformation. The modified casting process along with the Sr-modification has shown better grain refinement and eutectic Si modification than those achieved in the conventional cast alloys along with the Sr-modifier. These changes in microstructure in case of the modified cast alloys has led to an improvement in impact properties and wear resistance over the conventional cast alloys. The average impact energy of the alloys prepared through the modified casting process along with Sr modification has increased by approx. 107% and the average specific wear rate has reduced by approx. 54% compared to those of the only conventional cast alloys, respectively.

Keywords LM25 · Modified casting · Conventional casting · Sr-modifier · Impact energy · Wear rate

1 Introduction

Among various Al–Si alloys, LM25 alloy is one of the most preferred alloys in automotive and aerospace sector because of its high strength to weight ratio. LM25 alloy is being used in alloy wheels, chassis-related parts, and other engine and body castings [1]. These applications encourage to study

and improve the wear and impact properties of the alloys. Hypoeutectic Al–Si alloys prepared through conventional cast process (CCP) consists of large grains of α -Al and needle-like eutectic Si particles. These features attribute to poor mechanical properties in conventional cast alloys [1, 2]. Various studies have been conducted on the refinement of α -Al and modification of eutectic Si. Out of the many different ways, chemical treatments are primarily preferred in casting processes. Al–5Ti–1B and Sr based master alloys are normally used as grain refiners and modifiers, respectively in Al–Si alloy [3, 4]. However, these materials have their own process specific limitations. For example; the refining efficiency of Al–5Ti–1B decreases with increasing Si content above 3 wt.% because of posing phenomena [5, 6]. Similarly, Sr-based modifiers produce porosity in the material, and interaction between Sr and other alloying elements may lead to the formation of intermetallic phases that could reduce the modification effect [7, 8].

The modified casting process (MCP) can reduce the grain size of α -Al phase and modify the eutectic Si particles into short needle-like structure simultaneously, without any foreign additives. This modified casting process is termed as melt thermal treatment (MTT), mixed melt therapy, duplex casting process and melt thermal-rate treatment in different literatures. The mechanism of the modified casting process for hypoeutectic Al–Si alloy is proposed by Wang et al. [9, 10]. The concept of MCP is based on the fact that when a superheated melt (temperature ~ 200 °C above liquidus point) and a low temperature melt (temperature in between liquidus and solidus point) of same chemical composition are mixed, it creates many nucleation sites for the solidification of primary phase. Many researches have been conducted to determine the effect of modified casting process or similar treatments on microstructure and tensile properties of hypereutectic [11, 12] and hypoeutectic Al–Si alloys [10, 13–15]. The results

✉ Ajaya Kumar Pradhan
ajaya.meta@mnit.ac.in; 2017rmt9064@mnit.ac.in

¹ Department of Metallurgical and Materials Engineering,
MNIT Jaipur, Jaipur 302017, India

have confirmed that the MCP process can refine the primary Si particles in hypereutectic alloys and can also partial modify the eutectic Si. In hypoeutectic alloys, MCP can reduce the primary dendrite arm length and the average length of eutectic Si. These favorable changes in microstructure lead to an overall improvement in mechanical properties.

The first report on the effect of MTT process on hypoeutectic Al–Si alloy was made by Wang et al. [10]. They found that the MTT process refines primary dendrites of α -Al and modifies the morphology of intermediate Fe rich phases. These microstructural modifications significantly improve the mechanical properties of the alloy, especially ductility, which is enhanced by 46.2% than that of the conventional cast alloy. Chen et al. [15] have investigated the effect of superheat treatment on Al–7Si–0.55 Mg alloy. They found that the ultimate tensile strength and ductility of the alloy treated by superheat treatment improves by 11.5 and 41.12%, respectively, compared to that of the conventional cast alloy. However, to the best knowledge of the authors, no research has been conducted on the effects of MCP or similar treatments on impact and wear properties of A356 (LM25) alloy. The objective of this paper is thus to find out the effects of a modified casting process on toughness and wear resistance of LM25 alloy.

2 Experiment Procedure

In conventional casting process, LM25 alloys (procured from Kastwell foundries, India) were remelted at 720 °C in an electrical resistance muffle furnace. The alloy was degasified by adding C₂Cl₆ tablets into the melt. The modification was carried out by adding Al–5Sr master alloy (Sr ~ 200 ppm) into the melt. Finally, the prepared melt was poured into preheated (250 °C) graphite moulds of different dimensions for casting. Samples were also prepared without modification for comparison purpose.

In modified casting process, the melt was divided into two halves after melting at 720 °C (with or without Sr-modifier). In one half (high temperature melt (HTM)), the temperature was raised to 900 °C and was held there for 20 min. In other half (low temperature melt (LTM)), the temperature was decreased to 600 °C and was held there for 20 min. Then the high temperature melt was poured into the low temperature melt, followed by manual stirring using a graphite rod and pouring into preheated (250 °C) graphite mould for casting.

Chemical compositions of procured LM25 alloy and Al–5Sr master alloy as investigated by optical emission

spectrometer (OES) (Spectrolab, India) are given in Table 1. The sample codes and their descriptions are given in the Table 2. The prepared alloys were then went through sectioning, wet grinding and polishing. Further, samples were etched with Keller’s etchant (95% H₂O + 2.5% HNO₃ + 1.5% HCl + 1% HF) and Poulton’s etchant (60% HNO₃ + 30% HCl + 5% HF + 5% H₂O) for microstructural and macrostructural analysis, respectively. The microstructure of the alloys was captured with the help of an optical microscope (Zeiss Axio vert. A1) and the morphology of eutectic Si was analysed using ImageJ software. The macrostructure of the samples was observed using a stereomicroscope at 12× magnification and the grain size was analysed using ImageJ software.

Charpy test was conducted to determine the impact toughness of the prepared LM25 alloys. Cast samples were machined to 10 mm × 10 mm × 55 mm for this test. Two samples from each casting conditions were tested to ensure the reproducibility of the results. Fracture surface analysis of the impact test samples was carried out using a scanning electron microscope (FE-SEM, Nova Nano SEM 450).

Experimental density of prepared alloys was measured using Archimedes’ method. Vickers microhardness was measured at ten different positions of at least two different samples prepared under similar conditions using a load of 200 g and a dwell time of 15 s. Then the average of all the reading were calculated.

Dry sliding wear test of the prepared LM25 alloys was conducted using a pin on disc instrument (DUCOM, TR50). Samples of dimension (ø8 mm × 33 mm) were used for this purpose. The wear test parameters of each sample were fixed and are mentioned in Table 3. The test was conducted as per ASTM G 99-90 standards. Weight loss method was used to determine wear rate (WR) of the samples as given by the formula in Eq. 1.

$$\text{Wear rate (g/m)} = \frac{\Delta W \times 1000}{2\pi r.N.t} \tag{1}$$

Table 2 Prepared LM25 alloys under different casting conditions

Sample code	Description of casting condition
CC	Conventional casting process
MC	Modified casting process
MCC	Conventional casting process with Sr modifier
MMC	Modified casting process with Sr modifier

Table 1 Chemical composition of various procured material

Element	Si	Mg	Fe	Ti	Cu	Mn	Zn	V	B	Sr	Al
LM25 alloy	6.82	0.32	0.15	0.03	0.05	0.05	0.01	0.01	–	0.002	Bal
Al-5Sr	0.11	0.01	0.24	0.006	0.001	0.004	0.001	0.012	–	4.82	Bal

Table 3 Wear test parameters

Test parameter	Disc material	F (N)	N (rpm)	r (mm)	t (min.)	Temperature (°C)
Value	EN31 steel	10	100	40	15	25

where ΔW , r , t and N are weight loss (g), track radius (mm), time duration (min) and speed (rpm), respectively.

3 Results and Discussion

3.1 Microstructural Analysis

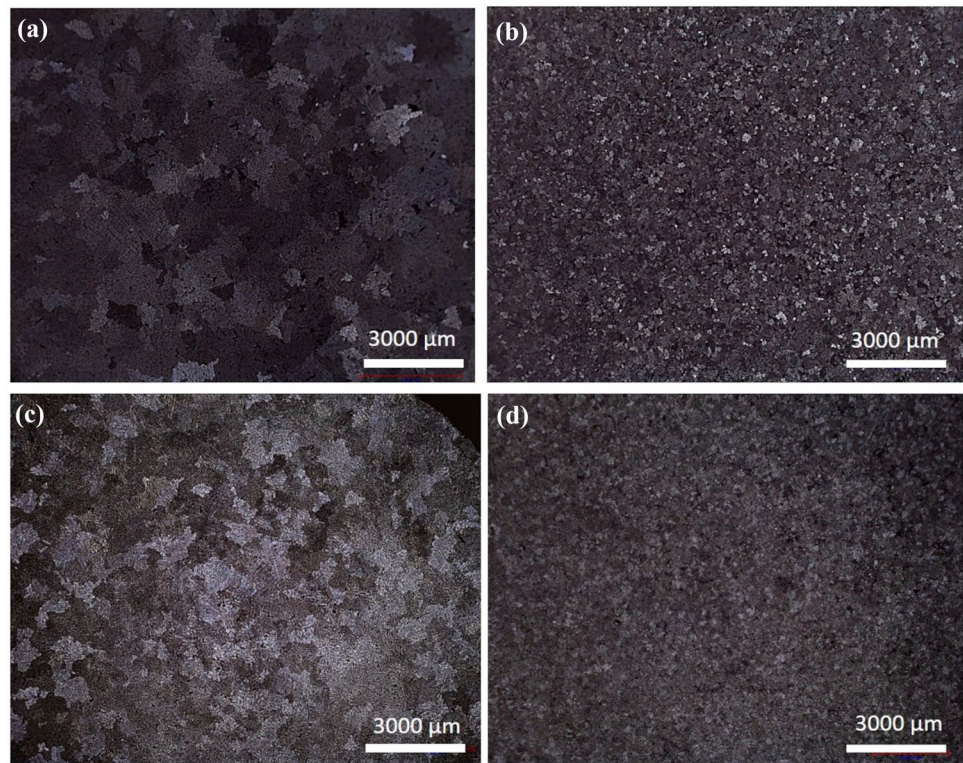
Figure 1 shows the effect of different processing methods on the macrostructure of A356 alloy. The macrostructures indicate that the MCP alloys (MC and MMC) have produced refined and equiaxed α -Al phase compared to the CCP alloys (CC and MCC alloy). This is because of intermixing of the HTM with the LTM in MCP, which creates many nucleation sites for the solidification of α -Al phase. Maximum grain size reduction is observed in case of the MMC alloy, which is approximately 50% less compared to the CC alloy. Wang et al. [10] have also found that MTT process (similar to MCP) reduces the average length of primary dendrite of α -Al and the shape of the grains change into equiaxed in A356 alloy.

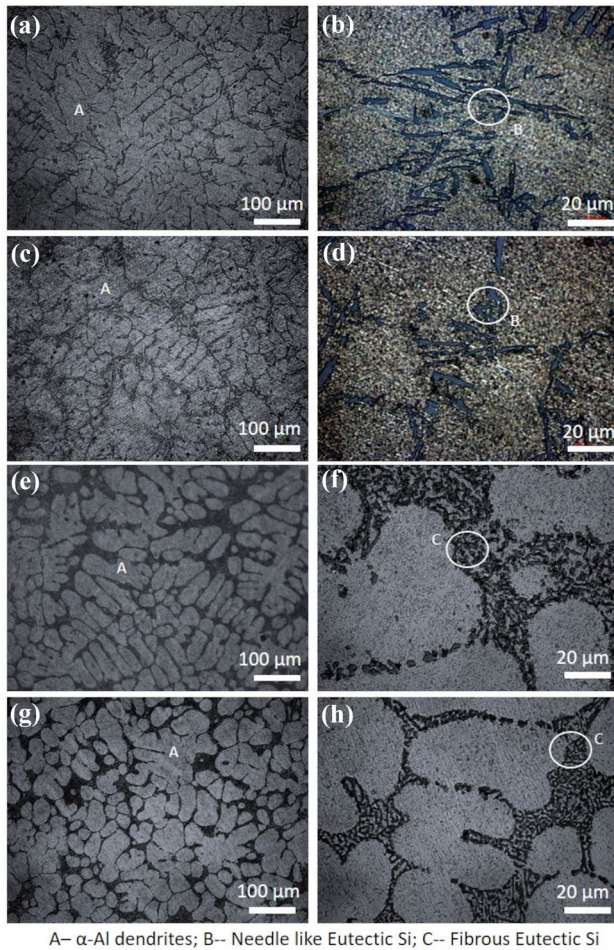
The corresponding variations in microstructure are shown in Fig. 2. From the microstructure, it may be observed that

each of the alloy consists of α -Al dendrites and needle like eutectic Si particles (Fig. 2b, d) and the structure is observed to be fibrous (Fig. 2f, h). However, length of primary dendrites (Fig. 2c) and eutectic Si particles are lesser in case of the MC alloy than in the CC alloy (Fig. 2a). There are no other changes in morphology of eutectic Si in the above two alloys. In case of the Sr-modified alloys (MCC and MMC), the morphology of eutectic Si gets converted into short rod-like and/or spherical shapes from needles-like shapes. When a modifier is added to the melt, the growth mechanism of eutectic Si changes, and is known as impurity induced twinning. According to this mechanism, atoms of Sr-modifier segregate at the interface of solid dendrites and eutectic liquid, and inhibit the growth of eutectic Si particles. Moreover, MMC alloy microstructure consists of finer globular cells of α -Al phase (Fig. 2g), unlike coarser dendrites in MCC alloy (Fig. 2e). This implies the breakage of dendrites after mixing of LTM and HTM melts in the MMC alloy.

Table 4 quantitatively summarizes the variation in microstructural features like, average grain size of α -Al and eutectic Si particles length of samples prepared through different casting conditions. The results indicate that not

Fig. 1 Macrostructure of **a** CC, **b** MC, **c** MCC and **d** MMC





A-- α -Al dendrites; B-- Needle like Eutectic Si; C-- Fibrous Eutectic Si

Fig. 2 Optical microstructure of a, b CC, c, d MC, e, f MCC, and g, h MMC

Table 4 Quantitative variation in microstructural features of A356 alloys

Sample	Grain size (μm)	Eutectic Si length (μm)
CC	821 \pm 45	23.9 \pm 5.3
MC	485 \pm 20	16.2 \pm 2.7
MCC	730 \pm 25	3.7 \pm 1.4
MMC	365 \pm 17	3.2 \pm 2.1

only the α -Al grains get refined, but also the average length of eutectic Si gets reduced significantly in the MC alloy. The percentage reduction in average grain size and eutectic Si particles length in case of the MC alloy is approx. 41 and 32.2% than that of the CC alloy, respectively. The average length of eutectic Si in MMC alloy is reduced by appx. 86 and 14% compared to that of the CC and MCC alloys, respectively. Similar observations have also been made by Samuel et al. [16] and have reported that MTT

leads to refinement in eutectic Si to a certain extent without any change in the morphology. Moreover, combination of MTT and Sr-modifier causes better modification of eutectic Si characteristics than the individual processes. MCP results in smaller dendritic cell structure and the eutectic mixture get solidified at the interdendritic region (between arm of α -Al). Smaller cells inherently restrict the growth of eutectic Si and hence lead to the refinement of eutectic Si in MCP alloys.

According to Wang et al. [10, 11], when the melt temperature is close to melting point of the alloy (in conventional casting process), several large solid-like atomic clusters of Si-Si, and Al-Si get formed in the melt and such structures are known as micro-inhomogeneous structure [17, 18]. The modified casting technique can change these micro-inhomogeneous structures into nanosize homogenous structures. When the melt temperature reaches 890–950 °C, larger-sized atomic clusters convert into small nanosized atomic clusters and the melt gets a uniform distribution of these clusters. These nano-sized homogenous structures can be retained at pouring temperature by mixing the low temperature alloy melt of the same composition. This mixing forms many small and uniformly distributed solid-like atomic clusters in the final melt which act as crystal nuclei for α -Al phases. Also, LTM has semi-solid content, which when mixed with HTM, forms free secondary dendritic arms. These free secondary dendritic arms also act as heterogeneous nucleation sites for α -Al. In both of the above mentioned ways, MCPs produce finer microstructure (Fig. 1b, d).

3.2 Impact Test Analysis

The variation in impact energy of A356 alloys prepared under different casting conditions are shown in Fig. 3. The results have revealed that among various alloys, the CC alloy exhibits lowest average impact energy (3.8 J/cm²), whereas the MMC alloy exhibits highest average impact energy (8.1 J/cm²). In case of the unmodified alloys, impact energy of the MC alloy is found to be higher than that of the CC alloy by 25.4%. In case of the modified alloys, impact energy of the MMC alloy is higher than that of CC and MCC alloy by 105 and 6.7%, respectively. Elahi et al. [19] have concluded that the impact energy of A356 alloy increases by 137% by Sr-modification. Samuel et al. [20] have found that when A356 alloy is treated with both Al-5Ti-1B grain refiner and Sr-modifier, the impact energy of the as-cast alloy reaches 13.81 J.

The variation in toughness (impact energy) in various alloys can be explained as follows. The size, shape and distribution (spacing between particles) of eutectic Si particles, and the grain size of α -Al are important parameters that affect the value of impact energy of cast Al-Si

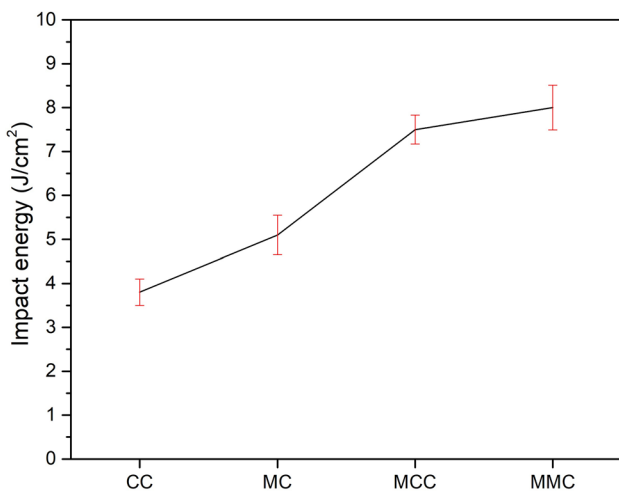


Fig. 3 Variation in impact energy in various alloys

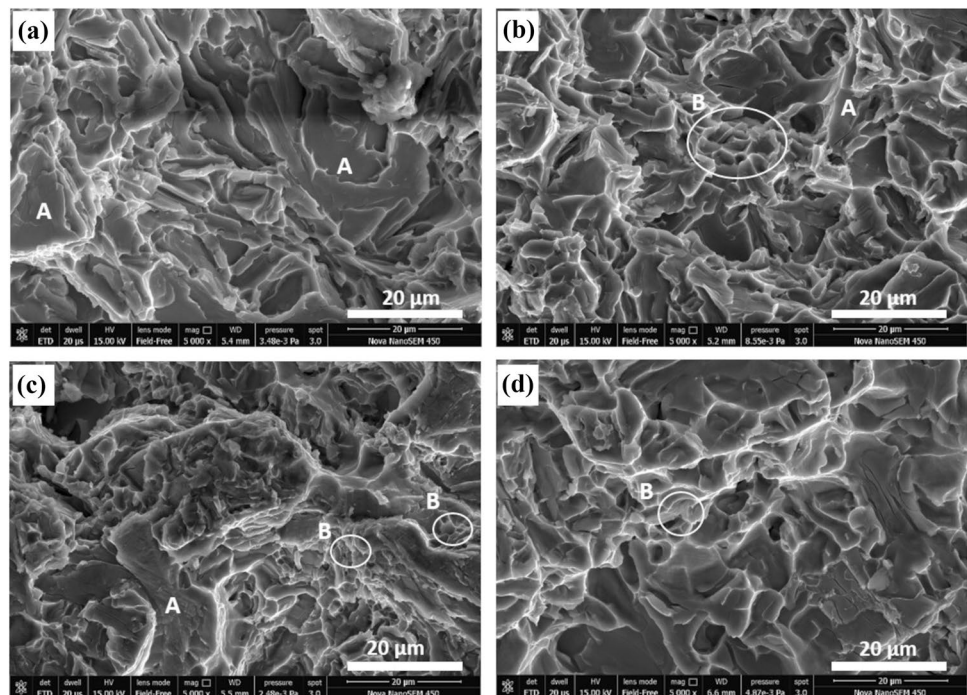
alloys [21]. The alloy having more refined and uniformly distributed phases is expected to have higher toughness. The unmodified alloys (CC and MC) consist of large grains of α -Al and needle-like eutectic Si particles in the microstructure as discussed in microstructure section. These needle like Si particles act as stress concentrator sites in the α -Al matrix. Hence, the toughness decreases. The large grain size of α -Al and large eutectic Si within the grains lead to a preferred and accessible way for transgranular crack propagation along the Si needles [22]. However, the MC alloy has a microstructure

consisting of relatively finer α -Al grains and shorter needles of Si which are responsible for better strength and ductility in MC over the CC alloy. This ultimately results in better toughness in MC alloy.

The morphological transformation in both the Sr-modified alloys (MCC and MMC) leads to lower stress concentration effect of Si particles and increase the interspacing between eutectic Si. Thus, cracks have to face more ductile phase (α -Al dendrites) during propagation [23]. Because of this, even though cracks may generate within the Si needles, transgranular crack propagation becomes difficult and results in inter-granular crack propagation along dendritic arms. Because of this, Sr-modified alloys have better toughness than unmodified alloys. Relative finer and better distribution of eutectic Si particles in MMC alloy results in slightly higher toughness than that of the MCC alloy.

SEM images of fractured impact test sample surfaces of various A356 alloys are shown in Fig. 4. The fractured surfaces of the unmodified alloys (CC and MC) show cleavage planes because of the presence of needle-like eutectic Si in the microstructure (Fig. 2a and b), which in turn creates brittleness in the alloy. In Al–Si alloy, eutectic Si is the preferred site for microcracks initiation. Once crack generates, it is followed by linkage of these cracks to adjacent cracks. This is known as Si-driven quasi cleavage fracture mode [22]. However, because of the presence of relatively finer α -Al grains (smaller SDAS) and shorter eutectic Si particles in the MC alloy (Fig. 2c-d), small microvoids (dimples fracture mode) are found at

Fig. 4 SEM images of A356 alloys prepared under different conditions, **a** CC, **b** MC, **c** MCC and **d** MMC. (A: Cleavage planes, B: Dimples/microvoids)



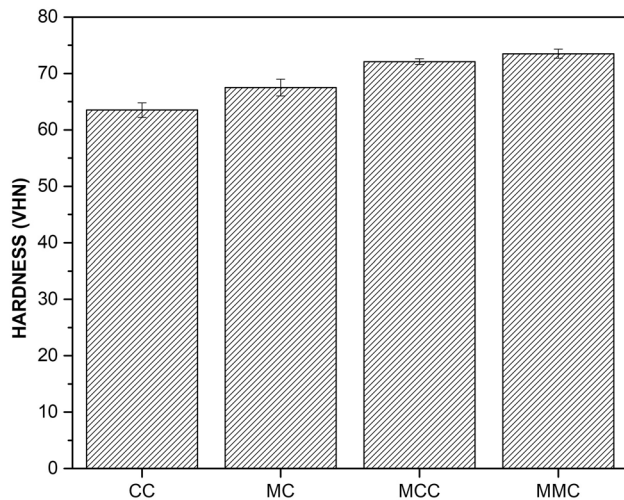


Fig. 5 Variations in hardness of various A356 alloys

some place in the fractured surface of that alloy (Fig. 5b). In Sr-modified alloys (MCC and MMC), the fractured surfaces indicate a mixed mode of fracture (dimple and cleavage) because of the presence of modified eutectic Si particles in the microstructure. This indicates that the toughness of modified alloys is better than that of the unmodified alloys, which justifies the impact test results.

3.3 Wear Test Analysis

Wear resistance depends on hardness and porosity of alloy. An increment in porosity in alloy, increase wear rate of alloy as the pores decrease the strength and hardness of the alloy along with decreasing the real area of contact during wear test. In the present work, density of various prepared cast alloys is found to be in between 2.58 and 2.61 g/cm³ that is close to the theoretical density of LM25 alloy (2.65 g/cm³). This indicates that the porosity content of the prepared alloys ranges between 1.8 and 4.1%. It confirms that effect of porosity content is negligible on wear rate of alloys.

Variation in hardness (VHN) of various cast alloys is illustrated in Fig. 5. The data obtained for different casting conditions of LM25 alloys reveal that MCP processed alloys (MC and MMC) exhibit higher hardness compared to the conventional cast alloys (CC and MCC). The VHN of MMC alloy is increased by 15.7 and 2%, respectively, over the CC alloy and MCC alloy, respectively.

The pin on disc test outcomes of various A356 alloys are illustrated in Fig. 6. The results have revealed that the wear resistance of the as cast A356 alloys (both Sr-modified and unmodified) prepared by the modified casting process is higher than that prepared by conventional casting process. The wear rate (WR) of the MC alloy is 33.6% less than that of the CC alloy. The reason behind this observation is the

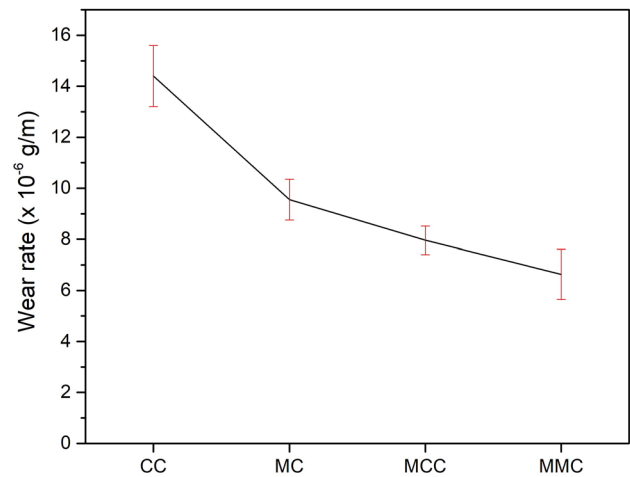


Fig. 6 Variations in wear rate of various A356 alloys

refined grains of α -Al in case of the MC alloy which not only results in higher hardness, but also leads to faster strain hardening during wear test. It is also found that the sample prepared by the combination of modified casting process and Sr-modification (MMC alloy) results in lowest wear rate than the samples prepared by individual processes. The wear rate of the MMC sample is lower than the CC, MC and MCC samples by 53.9, 30.5 and 16.7%, respectively. This is because the MMC alloy has the finest equiaxed α -Al grains among all the alloys. Moreover, MMC alloy consists of relatively fine and more uniformly distributed modified eutectic Si particles within the matrix. These features lead to higher hardness and wear resistance in the MMC alloy. In one of their research, Lee et al. [24] have also revealed that because of the morphological conversion brought about by the Sr-modifier in the A356 alloy, the stress concentration sites reduce and the wear resistance increases. Pramod [25] and Prasad [26] have investigated the effect of Scandium and Strontium modifier, respectively, on wear rate of A356 alloy. They have concluded that the addition of modifiers decreases the wear rate of alloy by morphological transformation of the eutectic Si particles.

Worn out surfaces of different A356 alloys are shown in Fig. 7. The presences of ploughing grooves and oxide layer in each alloy confirm abrasive wear mechanism [27]. The hardness of surface plays an important role in abrasive wear. In case of the CC alloys (Fig. 7a), deep grooves get formed because of entrapped debris between the alloy and the disc (ploughing). However, relatively fine grooves are present in case of MC alloy (Fig. 7b) because of its higher hardness owing to refinement of α -Al.

In case of Sr-modified alloys (Fig. 7c, d), the surface show lesser abrasive wear of oxide layer because of the improvement in strength and hardness because of better refinement and modification of the microstructure. Also,

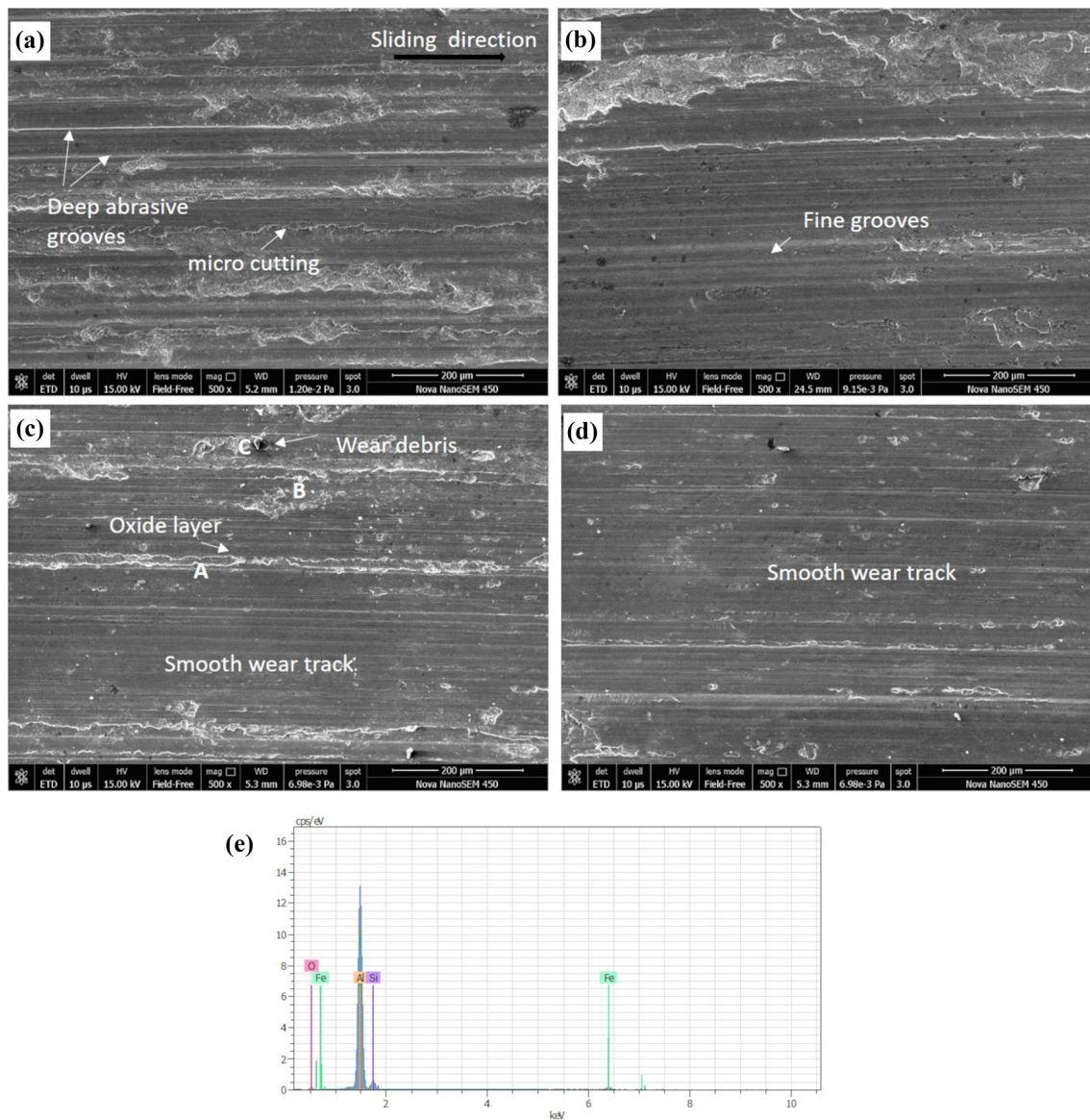


Fig. 7 SEM images of worn surface of A356 alloys prepared under different conditions, **a** CC, **b** MC, **c** MCC and **d** MMC, **e** EDS spectrum of MCC

the strain hardening rate is expected to be higher in these alloys during the wear test because of their small grain size and modified eutectic Si. These ultimately result in higher wear resistance as observed in the test (Fig. 6). Chandrashekharaiah et al. [28] have found out that adhesive wear occurs in Al–12Si alloy without any grain refiner and modifier. However, abrasive groove and oxide layer comes into play with the addition of grain refiner and modifier in that alloy.

The detached materials namely, Al, Si from A356 alloy and Fe from the counter disk, form a mechanically mixed layer (oxide layer) because of the presence of higher temperature. The presence of oxide layer in worn out

alloys are confirmed by EDS spectrum of the MCC alloy (Fig. 7c). Effect of oxide layer on wear resistance depends on the thickness, structure, constitute and the bonding of the layer to the underlying material. The oxide layer may improve wear resistance of an alloy by reducing the friction at the interface when it has sufficient thickness, hardness and is stable. If the layer is too thick and is unstable, it may lead to more wear because of the breakage of the layer and subsequent oxidation-wear/wear-oxidation mechanism. Rajesh et al. [29] have concluded that the development of a hard adherent mechanically mixed layer (stable, thin) will provide best resistance to wear.

4 Conclusions

- The macrostructural analysis of the prepared samples confirm that the modified casting process (MC and MMC) produce refined and equiaxed α -Al phase compared to conventionally cast alloys (CC and MCC alloy).
- In the case of the Sr-modified alloys (MCC and MMC), the morphology of eutectic Si gets converted into short rod-like and/or spherical shapes from needle-like shapes (CC and MC alloys). However, the microstructure of MMC alloy consists of fine globular cells of α -Al phase, unlike coarser dendrites in MCC alloy. This implies the breakage of dendrites after mixing of the melts in MMC alloy.
- Morphological transformation in both the Sr-modified alloys (MCC and MMC) lowers the stress concentration effect by the Si particles and increases the interspacing between eutectic Si particles.
- The above two microstructural features attribute to highest impact energy and lowest wear rate in the MMC alloy than other alloys.
- Worn out surface of MMC alloy has shown finer groove and less damaged surface. This is because of the improvement in strength and hardness with refinement and modification in microstructure.

References

1. Pramod S L, Rao A K P, Murty B S, and Bakshi S R, *Mater Sci Eng A* **674** (2016) 438. <https://doi.org/10.1016/j.msea.2016.08.022>
2. Gupta R, Sharma A, Pandel U, and Ratke L, *Int J Cast Met Res* **30** (2017) 283. <https://doi.org/10.1080/13640461.2017.1299394>
3. Kumar G S V, Murty B S, and Chakraborty M, *J Alloy Compd* **472** (2009) 112. <https://doi.org/10.1016/j.jallcom.2008.04.095>
4. Prasada Rao A K, Das K, Murty B S, and Chakraborty M, *Mater Lett* **62** (2008) 273. <https://doi.org/10.1016/j.matlet.2007.05.020>
5. Birol Y, *Mater Sci Technol* **28** (2012) 385. <https://doi.org/10.1179/1743284711Y.0000000049>
6. Li Y, Hu B, Liu B, Nie A, Gu Q, Wang J, and Li Q, *Acta Mater* **187** (2020) 51. <https://doi.org/10.1016/j.actamat.2020.01.039>
7. Nampoothiri J, Balasundar I, Murty B S, and Ravi K R, *Mater Sci Eng A* **724** (2018) 586. <https://doi.org/10.1016/j.msea.2018.03.069>
8. Eguskiza S, and Niklas A, Fernandez-Calvo A I. *Santos F and Djurdjevic M, Inter Metalcast* **9** (2015) 43. <https://doi.org/10.1007/BF03355622>
9. Wang J, He S, Sun B, Zhou Y, Guo Q, and Nishio M, *Int J Cast Met Res* **14** (2001) 165. <https://doi.org/10.1080/13640461.2001.11819435>
10. Wang J, He S, and Sun B, *Mater Sci Eng A* **338** (2002) 101. [https://doi.org/10.1016/S0921-5093\(02\)00067-9](https://doi.org/10.1016/S0921-5093(02)00067-9)
11. Liang C, Chen Z H, Huang Z Y, and Zu F Q, *Mater Sci Eng A* **690** (2017) 387. <https://doi.org/10.1016/j.msea.2017.03.016>
12. Al-Helal K, Stone I C, and Fan Z, *Trans Indian Inst Metals* **65** (2012) 663. <https://doi.org/10.1007/s12666-012-0171-4>
13. Samuel A M, Garza-Elizondo G H, Doty H W, and Samuel F H, *Mater Des* **80** (2015) 99. <https://doi.org/10.1016/j.matdes.2015.05.013>
14. Jia P, Zhang J, Hu X, Teng X, Zuo M, Gao Z, Yang C, and Zhao D, *Mater Res Express* **5** (2018) 066520. <https://doi.org/10.1088/2053-1591/aac994>
15. Chen ZW, Jie WQ, Zhang RJ, *Mater Lett* **59** (2005) 2183–2185. <https://doi.org/10.1016/j.matlet.2004.08.047>
16. Samuel A M, Samuel F H, Doty H W, and Valtierra S, *Inter Metalcast* **11** (2017) 475. <https://doi.org/10.1007/s40962-016-0089-4>
17. Bian X F, and Wang W, *Mater Lett* **44** (2000) 54. [https://doi.org/10.1016/S0167-577X\(00\)00011-2](https://doi.org/10.1016/S0167-577X(00)00011-2)
18. Zu F Q, *Metals* **5** (2015) 395. <https://doi.org/10.3390/met5010395>
19. Elahi M A, and Shabestari S G, *Trans Nonferrous Met Soc China* **26** (2016) 956. [https://doi.org/10.1016/S1003-6326\(16\)64191-2](https://doi.org/10.1016/S1003-6326(16)64191-2)
20. Samuel A M, Doty H W, Valtierra S, and Samuel F H, *J Mater Des* **56** (2014) 264. <https://doi.org/10.1016/j.matdes.2013.10.029>
21. Casari D, Ludwig T H, Merlin M, Arnberg L, and Garagnani G L, *J Mater Eng Perform* **24** (2015) 894. <https://doi.org/10.1007/s11665-014-1355-3>
22. Shivkumar S, Wang L, and Keller C, *J Mater Eng Perform* **3** (1994) 83. <https://doi.org/10.1007/BF02654503>
23. Kumari S S S, Pillai R M, and Pai B C, *Mater Sci Eng A* **460–461** (2007) 561. <https://doi.org/10.1016/j.msea.2007.01.082>
24. Lee S, Cheng Y, and Chen W, *Lee C and Tan A Mater Chem Phys* **135** (2012) 503. <https://doi.org/10.1016/j.matchemphys.2012.05.015>
25. Pramod S L, Rao A K P, Murty B S, and Bakshi S R, *Mater Des* **78** (2015) 85. <https://doi.org/10.1016/j.matdes.2015.04.026>
26. Prasada Rao A K, Das K, Murty B S, and Chakraborty M, *Wear* **261** (2006) 133. <https://doi.org/10.1016/j.wear.2005.09.012>
27. Gupta R, and Sharma A, Pandel U and Ratke. *L Mater Res Express* **4** (2017) 046503. <https://doi.org/10.1088/2053-1591/aa680c>
28. Chandrashekharaiah T M, and Kori S A, *Tribology* **42** (2009) 59. <https://doi.org/10.1016/j.triboint.2008.05.012>
29. Rajesh A M, Kaleemulla K M, Saleemsab D, and Bharath K N, *SN Appl Sci* **1** (2019) 860. <https://doi.org/10.1007/s42452-019-0906-5>

Publisher’s Note Springer Nature remains neutral with regard to jurisdictional claims in published maps and institutional affiliations.

Springer Nature or its licensor (e.g. a society or other partner) holds exclusive rights to this article under a publishing agreement with the author(s) or other rightsholder(s); author self-archiving of the accepted manuscript version of this article is solely governed by the terms of such publishing agreement and applicable law.